(Preprint) AAS 23-014

BATCH DILUTION OF PRECISION OPTIMAL NAVIGATION PLANNING FOR CISLUNAR ENVIRONMENTS

Quinn Moon[*], David K. Geller[†]

Nova-C is a lunar lander developed by the private company Intuitive Machines to deliver commercial payloads to the Moon. The IM-1 mission set for 2023 will launch and land the Nova-C near the Moon's south pole. In this paper, Batch Dilution of Precision (DOP) methods are explored to assess Orbit Determination (OD) performance based on the nominal IM-1 trajectory. DOP has been traditionally used for time-instance measurements from one measurement type. This paper lays out the methodology to derive and incorporate a recursive, time-series DOP algorithm with both range and range-rate measurement data, in which a unitless PDOP is explicitly derived by utilizing a range to range-rate measurement error ratio. The DOP methods are used within a genetic algorithm optimizer to determine ground station tracking schedules that optimize OD performance. An assessment of OD performance is studied for key mission events including trajectory correction maneuvers (TCMs), lunar orbit insertion (LOI), and descent orbit insertion (DOI). The long-term goal of this research is to develop a fully integrated DOP and Linear Covariance Analysis optimization tool to minimize operational costs and maximize OD performance.

INTRODUCTION

A critical element of the IM-1 mission is Orbit Determination (OD) performance. Orbit Determination is the process of incorporating measurements to determine a spacecraft's state.[1] Navigation and guidance algorithms work together to provide accurate state estimates and subsequent targeting maneuvers for mission success. Associated with state estimation are state estimation errors, quantified traditionally with the state error covariance. Minimizing the state estimation covariance increases the reliability of guidance targeting algorithms and mission success.

Batch Least-Squares state estimation solutions have been used for a variety of inner and outer solar system missions including: the Apollo missions,[2] the Mariner missions to Venus and Mercury,[3] the Galileo mission to Jupiter,[4] and the Cassini mission to Saturn and its moons.[5] Further work has been done by Battin to derive a Least-Squares solution for nonlinear systems, a weighted Least-Squares solution for systems with measurement noise, and methods to recursively update the optimal estimate.[6]

A key factor for Least-Squares solutions is the measurement geometry. The quality of the measurement geometry can be measured using Dilution of Precision (DOP). Traditionally used for GPS systems, DOP provides a metric that can be used to study the measurement geometry of various estimation problems.[7,8]

[*]Graduate Student, Mechanical and Aerospace Engineering, Utah State University, North Logan, UT, 84341
[†]Professor, Mechanical and Aerospace Engineering, Utah State University Space Dynamics Laboratory, 416E Innovation Avenue, North Logan, UT, 84341

The IM-1 mission relies on range and range-rate measurements from various ground stations to perform OD analysis. The purpose of this paper is to determine which ground stations to use and when to use them for key OD segments, resulting in an optimal ground station tracking schedule. The optimal schedule reduces state estimation errors, quantified using DOP methods. This paper outlines the IM-1 mission and its OD segments, the formulation of a recursive DOP algorithm that incorporates measurement data from two measurement types, and the generation of the optimal ground station tracking schedule using a genetic algorithm.

REFERENCE TRAJECTORY AND OD SEGMENTS

The IM-1 reference trajectory and maneuvers in the J2000, Earth-Centered Inertial (ECI) coordinates are shown in Fig. 1. The nominal trajectory is generated by NASA's Copernicus software with midcourse correction maneuvers planned by Intuitive Machines.

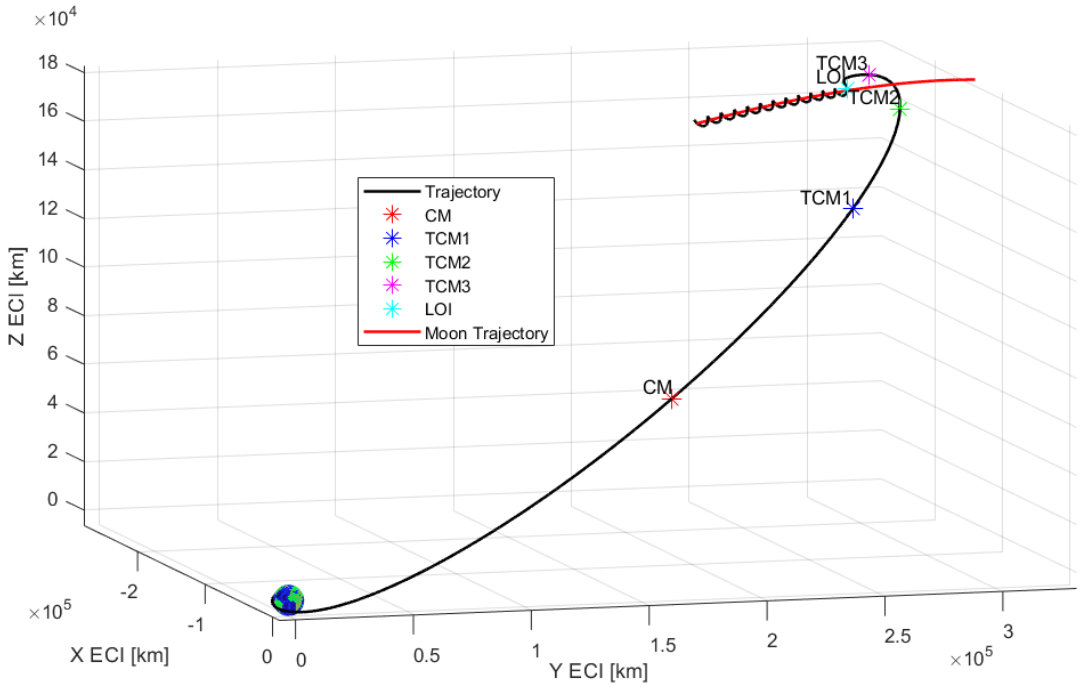

Figure 1: Nominal Cislunar Trajectory

The trajectory shown in Fig. 1 begins as the Nova-C lander separates from SpaceX's launch vehicle, referred to as Launch Vehicle Separation (LVS). The trajectory is then divided using midcourse corrections. These midcourse corrections consist of a larger Commissioning Maneuver (CM) and three smaller Trajectory Correction Maneuvers (TCMs). The Nova-C lander is inserted into lunar orbit with a Lunar Orbit Insertion maneuver (LOI). After several lunar orbits, the Nova-C lander begins a Descent Orbit Insertion maneuver (DOI) and descends to the lunar surface.

In addition to correcting Nova-C's trajectory, the maneuvers are utilized to separate the trajectory into subsections for state estimation analysis, referred to as OD segments. Each OD segment is analyzed separately to determine an optimal ground station tracking schedule that minimizes state estimation errors in preparation for an upcoming maneuver. In cislunar space, the OD segments

are further divided into subsegments in order to provide intermediate state estimates on an approximately daily basis. The OD subsegments help the optimization algorithm focus on one single rotation of the Earth and the corresponding visible stations. Furthermore, an accurate and precise state estimate is desired operationally by the ground navigation team in order to determine any anomalies during the mission. From LOI to DOI, the OD segment is broken up into six OD subsegments to provide a state estimation solution every two orbits, where each orbit takes approximately two hours.

GROUND STATION VISIBILITY

The optimal ground station tracking schedule is based on the visibility from 10 stations: Parkes, Australia (DSS49); Hartebeesthoek, South Africa (HBK26); Mauritius, Republic of Mauritius (MA1); Singapore (SI1); Kourou, French Guiana (KRU1); Byalulu, India (D32); Dubai, UAE (DU1); Okinwawa, Japan (OKN2); Morehead, Kentucky (DSS17); Goonhilly, England (GHY6).

Figure 2 below depicts when the stations are visible over a 48 hour period, based on the nominal trajectory from CM to TCM1. The pattern is near periodic as the Earth rotates and station visibility repeats. Three stations, MA1, SI1, and DU1, are specialized for Low Earth Orbits and are only visible for the first portion of the flight trajectory prior to LVS. Thus these three stations do not appear in the visibility report depicted in Fig. 2.

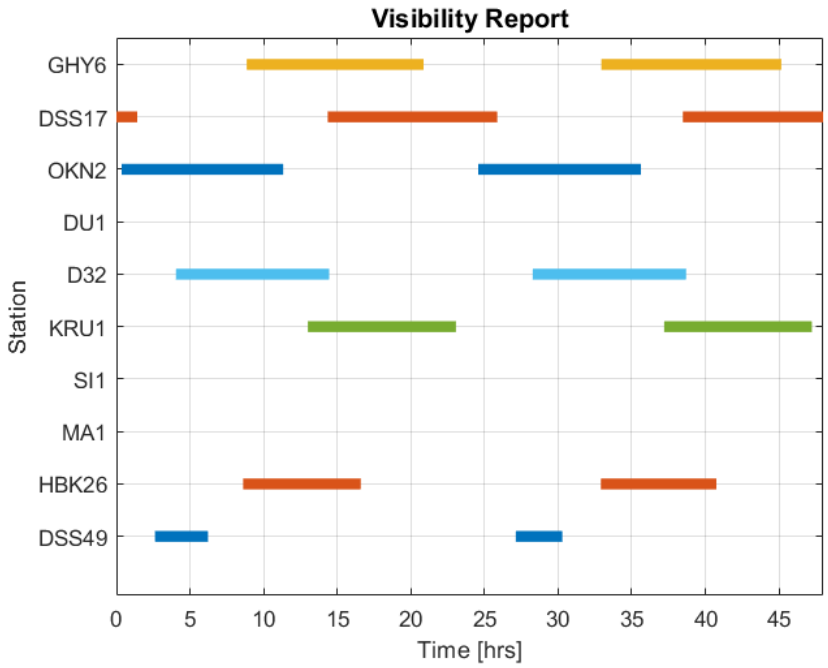

Figure 2: Visibility Report

FORMULATE DILUTION OF PRECISION ALGORITHM

Nonlinear Dynamics and Measurement Equations

The state vector $\boldsymbol{x}$ to be estimated using the DOP algorithm consists of Nova-C's position and velocity in J2000 inertial coordinates:

$$\boldsymbol{x} = \begin{bmatrix} \boldsymbol{r} \\ \boldsymbol{v} \end{bmatrix}$$

Additional states could be included to better model the system dynamics. However, these states are not the focus of the optimization problem and are not included in this study.

The dynamics used in the DOP algorithms are based on the nonlinear, point mass gravitational forces due to the Earth, Moon, and Sun. A study done by the author and Intuitive Machines comparing cislunar estimation errors based on a high fidelity, spherical harmonic Monte Carlo analysis and a point mass Linear Covariance analysis, achieved by linearizing the states about the nominal trajectory and analyzing a linearized Kalman filter, showed that inertial estimation errors match to within 2.64% in cislunar space and to within 13.43% in lunar orbit.[9] Future work will be done to incorporate higher order, spherical harmonic gravity models for the Earth and Moon, but are not expected to impact the optimal ground station tracking schedule. The vector differential equation modeling the system dynamics is expressed below:

$$\dot{\boldsymbol{x}}(t) = \boldsymbol{f}(\boldsymbol{x}(t), t) \tag{1}$$

The vehicle dynamics are linearized and discretized. Lear's method is used to calculate an approximate value of the State Transition Matrix:[10]

$$\boldsymbol{F} = \frac{\partial \boldsymbol{f}}{\partial \boldsymbol{x}} \tag{2}$$

$$\Delta t = t_{i+1} - t_i \tag{3}$$

$$\boldsymbol{\Phi}_{i+1,i} \approx \boldsymbol{I} + (\boldsymbol{F}_i + \boldsymbol{F}_{i+1})\frac{\Delta t}{2} + \boldsymbol{F}_i \boldsymbol{F}_{i+1}\frac{(\Delta t)^2}{2} \tag{4}$$

The discrete nonlinear measurement equation, including measurement noise, is expressed as:

$$\boldsymbol{z}_i = \boldsymbol{h}(\boldsymbol{x}_i, t) + \boldsymbol{\nu}_i \tag{5}$$

The measurement equation is linearized:

$$\boldsymbol{H} = \frac{\partial \boldsymbol{h}}{\partial \boldsymbol{x}} \tag{6}$$

$$\delta \boldsymbol{z}_i = \boldsymbol{H}\delta \boldsymbol{x}_i + \boldsymbol{\nu}_i \tag{7}$$

where $\boldsymbol{H}$ is referred to as the measurement partial matrix.

Generalized Dilution of Precision

Dilution of Precision is a Batch Least-Squares method for navigation analysis. Traditionally used to analyze several measurements at one instance, the equation can be modified to analyze a time series of measurement data that estimates the state at the final time t_n.[8] Expressing n linearized measurements in vector notation:

$$\delta \boldsymbol{z} = \begin{bmatrix} \boldsymbol{H}_0 \boldsymbol{\Phi}_{0,n} \\ \boldsymbol{H}_1 \boldsymbol{\Phi}_{1,n} \\ \vdots \\ \boldsymbol{H}_n \end{bmatrix} \delta \boldsymbol{x}_n + \boldsymbol{\nu} \tag{8}$$

Denoting the stacked matrix consisting of the measurement partials and the state transition matrices as $\boldsymbol{A}$, the Least-Squares estimate is found using the measurement data:[6,11]

$$\boxed{\delta \hat{\boldsymbol{x}} = \left(\boldsymbol{A}^T \boldsymbol{A}\right)^{-1} \boldsymbol{A}^T \delta \boldsymbol{z}} \tag{9}$$

The state error covariance is formulated using the linearized state estimate:

$$\boldsymbol{P}_{\delta \boldsymbol{x}_n} = E\left[(\delta \boldsymbol{x}_n - \delta \hat{\boldsymbol{x}}_n)(\delta \boldsymbol{x}_n - \delta \hat{\boldsymbol{x}}_n)^T\right] \tag{10}$$

The linearized measurement $\delta \boldsymbol{z}$ in Eq. 8 is substituted into Eq. 9:

$$\delta \hat{\boldsymbol{x}}_n = \left(\boldsymbol{A}^T \boldsymbol{A}\right)^{-1} \boldsymbol{A}^T (\boldsymbol{A} \delta \boldsymbol{x}_n + \boldsymbol{\nu}) \tag{11}$$

The difference between the Least-Squares estimate $\delta \hat{\boldsymbol{x}}_n$ and the linearized state $\delta \boldsymbol{x}_n$ is taken and substituted into Eq. 10

$$\delta \boldsymbol{x}_n - \delta \hat{\boldsymbol{x}}_n = -\left(\boldsymbol{A}^T \boldsymbol{A}\right)^{-1} \boldsymbol{A}^T \boldsymbol{\nu} \tag{12}$$

$$\boldsymbol{P}_{\delta \boldsymbol{x}_n} = E\left[\left(\boldsymbol{A}^T \boldsymbol{A}\right)^{-1} \boldsymbol{A}^T \boldsymbol{\nu} \boldsymbol{\nu}^T \boldsymbol{A} \left(\boldsymbol{A}^T \boldsymbol{A}\right)^{-1}\right] \tag{13}$$

The expectation of $\boldsymbol{\nu}^T \boldsymbol{\nu}$ is expressed as the strength of the measurement noise, assuming the measurement errors are equivalent between stations:

$$E[\boldsymbol{\nu} \boldsymbol{\nu}^T] = \boldsymbol{R} = \sigma_\nu^2 \boldsymbol{I} \tag{14}$$

The scalar value σ_ν^2 can be factored out of the expectation operator:

$$\boldsymbol{P}_{\delta \boldsymbol{x}_n} = \sigma_\nu^2 E\left[\left(\boldsymbol{A}^T \boldsymbol{A}\right)^{-1} \boldsymbol{A}^T \boldsymbol{A} \left(\boldsymbol{A}^T \boldsymbol{A}\right)^{-1}\right] \tag{15}$$

$$\boxed{\boldsymbol{P}_{\delta \boldsymbol{x}_n} = \sigma_\nu^2 \left(\boldsymbol{A}^T \boldsymbol{A}\right)^{-1}} \tag{16}$$

Thus the state estimation error covariance is represented at the final time using the Batch Least-Squares solution. For optimization algorithms, it is convenient to provide a single value that is to be optimized, known as the objective function. Position Dilution of Precision (PDOP) is formulated

by taking the square root of the trace of the position variances:

$$\boldsymbol{M_r} = \begin{bmatrix} \boldsymbol{I} \\ \boldsymbol{0} \end{bmatrix} \tag{17}$$

$$\text{RSS}(\boldsymbol{P}_{\delta \boldsymbol{r}_n}) = \sqrt{\text{tr}\left[\boldsymbol{M_r}^T \left(\sigma_\nu^2 \left(\boldsymbol{A}^T \boldsymbol{A}\right)^{-1}\right) \boldsymbol{M_r}\right]} \tag{18}$$

$$\text{RSS}(\boldsymbol{P}_{\delta \boldsymbol{r}_n}) = \sigma_\nu \sqrt{\text{tr}\left[\boldsymbol{M_r}^T \left(\boldsymbol{A}^T \boldsymbol{A}\right)^{-1} \boldsymbol{M_r}\right]} \tag{19}$$

$$\boxed{\text{RSS}(\boldsymbol{P}_{\delta \boldsymbol{r}_n}) = \sigma_\nu \text{PDOP}} \tag{20}$$

Note how PDOP acts as a multiplying factor independent to the measurement noise. Smaller PDOP values indicate better measurement geometry, resulting in smaller state estimation errors. Thus, PDOP provides an intuitive metric to quantify the dynamic measurement geometry between the stations and the spacecraft, and is used as the objective function in optimizing the ground station tracking schedule. Furthermore, for the case where σ_ν pertains to range measurements, PDOP is unitless.

Another common metric in DOP analysis is Velocity Dilution of Precision (VDOP), where the trace of velocity variances are analyzed. For the case where σ_ν pertains to range measurements, VDOP has units of $\frac{1}{s}$, which is more arbitrary for analyzing the dynamic measurement geometry. However, for the case where σ_ν pertains to range-rate measurements, VDOP is unitless and PDOP has units of s, making VDOP the more intuitive metric.

It is important to note that the optimal ground tracking schedules found in this research are optimal with respect to PDOP, not VDOP. PDOP is chosen as the primary objective function to be minimized since it is the more common unitless metric for DOP analysis. Furthermore, a tracking schedule that yields higher velocity estimation errors will directly cause higher position estimation errors over time through error propagation. Thus, while tracking schedules that are optimal with respect to PDOP are not strictly optimal with respect to VDOP, it can be safely assumed that the optimal PDOP schedule produces an acceptable VDOP. Before the tracking schedule is implemented in real time, an analysis should be performed to verify whether the PDOP and VDOP values are acceptable to mission requirements.

Computational Efficiency and Recursive Methods

It can become computationally burdensome to continually increase the size of $\boldsymbol{A}$ and calculate $\boldsymbol{A}^T\boldsymbol{A}$ as measurements are incorporated. Thus, a recursive relationship is derived by studying how $\boldsymbol{A}^T\boldsymbol{A}$ evolves as additional measurements are taken. The matrix $\sigma_\nu^2 \boldsymbol{A}^T\boldsymbol{A}$ is called the information matrix. Since the measurement errors are independent of the station geometry, the matrix $\boldsymbol{A}^T\boldsymbol{A}$ is sometimes referred to as the geometry information matrix, or just the information. Below $\boldsymbol{A}^T\boldsymbol{A}$ is expressed for two measurements to estimate the state at time t_1:

$$\boldsymbol{A}_1 = \begin{bmatrix} \boldsymbol{H}_0 \boldsymbol{\Phi}_{0,1} \\ \boldsymbol{H}_1 \end{bmatrix} \tag{21}$$

$$\left[\boldsymbol{A}^T\boldsymbol{A}\right]_1 = \boldsymbol{H}_1^T\boldsymbol{H}_1 + \boldsymbol{\Phi}_{0,1}^T \boldsymbol{H}_0^T \boldsymbol{H}_0 \boldsymbol{\Phi}_{0,1} \tag{22}$$

Processing another measurement at time t_2:

$$\boldsymbol{A}_2 = \begin{bmatrix} \boldsymbol{H}_0\boldsymbol{\Phi}_{0,2} \\ \boldsymbol{H}_1\boldsymbol{\Phi}_{1,2} \\ \boldsymbol{H}_2 \end{bmatrix} \tag{23}$$

$$\left[\boldsymbol{A}^T\boldsymbol{A}\right]_2 = \boldsymbol{H}_2^T\boldsymbol{H}_2 + \boldsymbol{\Phi}_{1,2}^T\boldsymbol{H}_1^T\boldsymbol{H}_1\boldsymbol{\Phi}_{1,2} + \boldsymbol{\Phi}_{0,2}^T\boldsymbol{H}_0^T\boldsymbol{H}_0\Phi_{0,2} \tag{24}$$

Note that $\boldsymbol{A}^T\boldsymbol{A}$ with three measurements at time t_2 can be expressed in terms of $\boldsymbol{A}^T\boldsymbol{A}$ with two measurements at time t_1 by taking advantage of the fact that for state transition matrices $\boldsymbol{\Phi}_{0,2} = \boldsymbol{\Phi}_{0,1}\boldsymbol{\Phi}_{1,2}$:

$$\left[\boldsymbol{A}^T\boldsymbol{A}\right]_2 = \boldsymbol{H}_2^T\boldsymbol{H}_2 + \boldsymbol{\Phi}_{1,2}^T\left[\boldsymbol{A}^T\boldsymbol{A}\right]_1\boldsymbol{\Phi}_{1,2} \tag{25}$$

$$\boxed{\left[\boldsymbol{A}^T\boldsymbol{A}\right]_{i+1} = \boldsymbol{H}_{i+1}^T\boldsymbol{H}_{i+1} + \boldsymbol{\Phi}_{i,i+1}^T\left[\boldsymbol{A}^T\boldsymbol{A}\right]_i\boldsymbol{\Phi}_{i,i+1}} \tag{26}$$

Thus new measurement data can easily be incorporated by recursively updating $\boldsymbol{A}^T\boldsymbol{A}$. However, in order to calculate PDOP at each step, the inverse of $\boldsymbol{A}^T\boldsymbol{A}$ must be taken, which may be computationally difficult or impossible if the matrix is not full rank. To improve the robustness and avoid constantly taking the inverse of $\boldsymbol{A}^T\boldsymbol{A}$, the small-rank adjustment method for matrix inversion is implemented. The small-rank adjustment method outlines how to find the inverse of the sum of a rank-1 matrix and a full rank matrix:[11]

$$(\boldsymbol{X} + \boldsymbol{UCV})^{-1} = \boldsymbol{X}^{-1} - \boldsymbol{X}^{-1}\boldsymbol{U}\left(\boldsymbol{C}^{-1} + \boldsymbol{VX}^{-1}\boldsymbol{U}\right)^{-1}\boldsymbol{VX}^{-1} \tag{27}$$

Implementing the small-rank adjustment method to the recursive DOP equations:

$$\boldsymbol{\Gamma}_i = \left[\boldsymbol{A}^T\boldsymbol{A}\right]_i^{-1} \tag{28}$$

$$\boldsymbol{\Gamma}_{i+1}^- = \boldsymbol{\Phi}_{i+1,i}\boldsymbol{\Gamma}_i\boldsymbol{\Phi}_{i+1,i}^T \tag{29}$$

$$\boxed{\boldsymbol{\Gamma}_{i+1}^+ = \boldsymbol{\Gamma}_{i+1}^- - \frac{\boldsymbol{\Gamma}_{i+1}^-\boldsymbol{H}_{i+1}^T\boldsymbol{H}_{i+1}\boldsymbol{\Gamma}_{i+1}^-}{1 + \boldsymbol{H}_{i+1}\boldsymbol{\Gamma}_{i+1}^-\boldsymbol{H}_{i+1}^T}} \tag{30}$$

This recursive method does not involve any matrix inversion, except for the necessary initialization of $\boldsymbol{\Gamma}$, which is more efficient and leads to fewer computational errors. Note the denominator is a scalar value since measurements are incorporated from only one measurement source.

Condition Number Implementation

As mentioned, using the matrix inversion lemma is dependent on $\boldsymbol{A}^T\boldsymbol{A}$ being full rank, and thus invertible. However, given machine precision, the matrix inverse may not be accurate and could cause the DOP algorithm to become unstable, despite $\boldsymbol{A}^T\boldsymbol{A}$ being full rank. To avoid inaccuracies, a condition number tolerance is set in the DOP algorithm. Once the condition number is small enough for accurate inversion, the matrix $\boldsymbol{A}^T\boldsymbol{A}$ is inverted and the recursive method using $\boldsymbol{\Gamma}$ is used, as depicted below in Fig. 3

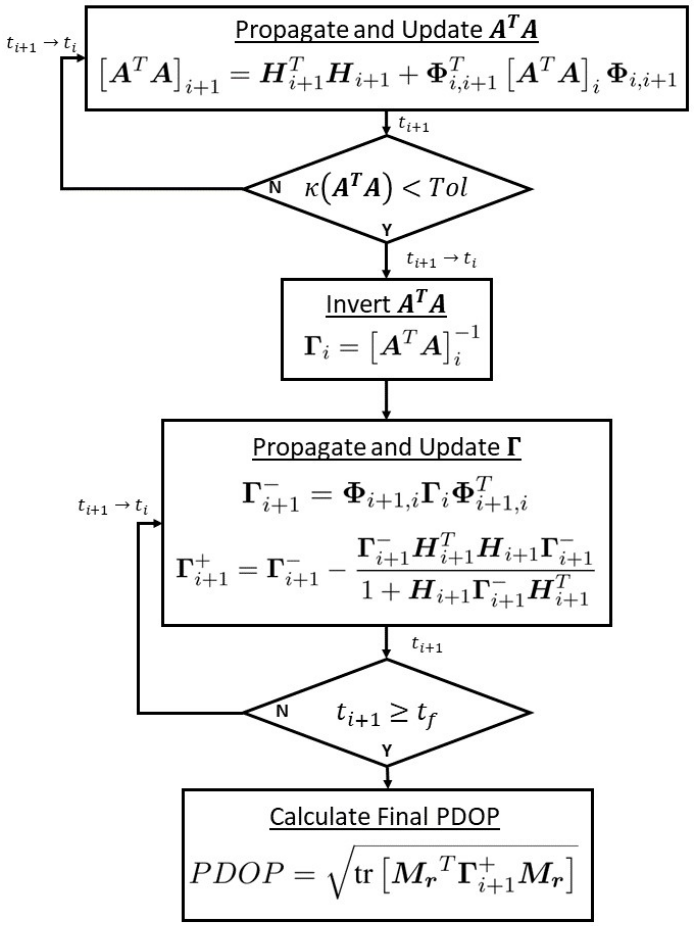

Figure 3: DOP Algorithm Flow Chart

The DOP algorithm runs, propagating and incorporating available measurements, to the end of the OD segment. The PDOP can be calculated at all times once the condition number tolerance is met, ensuring that the results are numerically accurate. If a contact schedule leads to the scenario where the condition number tolerance is never met, a large, default PDOP value is returned to indicate numerical inaccuracy.

DOP with Multiple Measurement Types

In the derivation of DOP, the expectation of the measurement noise was expressed as a scalar multiplied by the identity matrix. DOP has been restricted to one measurement type since the noise cannot simply be factored out of the expectation operator with multiple measurement types. Here a new Weighted Least-Squares DOP algorithm is derived that incorporates both range and range-rate measurements. A Weighted Batch Least-Squares solution is expressed as:[6]

$$\delta\hat{\boldsymbol{x}} = \left(\boldsymbol{A}^T\boldsymbol{W}\boldsymbol{A}\right)^{-1}\boldsymbol{A}^T\boldsymbol{W}\delta\boldsymbol{z} \tag{31}$$

where $\boldsymbol{W}$ is a weighting matrix. The state error covariance is again formulated using the linearized state estimate:

$$\boldsymbol{P}_{\delta\boldsymbol{x}_n} = E\left[(\delta\boldsymbol{x}_n - \delta\hat{\boldsymbol{x}}_n)(\delta\boldsymbol{x}_n - \delta\hat{\boldsymbol{x}}_n)^T\right] \tag{32}$$

The linearized measurement $\delta\boldsymbol{z}$ is substituted into the Least-Squares estimate in Eq. 31:

$$\delta\hat{\boldsymbol{x}}_n = \left(\boldsymbol{A}^T\boldsymbol{W}\boldsymbol{A}\right)^{-1}\boldsymbol{A}^T\boldsymbol{W}(\boldsymbol{A}\delta\boldsymbol{x}_n + \boldsymbol{\nu}) \tag{33}$$

The difference between the Least-Squares estimate $\delta\hat{\boldsymbol{x}}_n$ and the linearized state $\delta\boldsymbol{x}_n$ is taken and substituted into Eq. 32

$$\delta\boldsymbol{x}_n - \delta\hat{\boldsymbol{x}}_n = -\left(\boldsymbol{A}^T\boldsymbol{W}\boldsymbol{A}\right)^{-1}\boldsymbol{A}^T\boldsymbol{W}\boldsymbol{\nu} \tag{34}$$

$$\boldsymbol{P}_{\delta\boldsymbol{x}_n} = E\left[\left(\boldsymbol{A}^T\boldsymbol{W}\boldsymbol{A}\right)^{-1}\boldsymbol{A}^T\boldsymbol{W}\boldsymbol{\nu}\boldsymbol{\nu}^T\boldsymbol{W}\boldsymbol{A}\left(\boldsymbol{A}^T\boldsymbol{W}\boldsymbol{A}\right)^{-1}\right] \tag{35}$$

Here $\boldsymbol{\nu}$ is a random noise vector from both range and range-rate measurements. The expected value of $\boldsymbol{\nu}^T\boldsymbol{\nu}$ is expressed as $\boldsymbol{R}$, again assuming each station's measurement noises are equal:

$$\boldsymbol{P}_{\delta\boldsymbol{x}_n} = E\left[\left(\boldsymbol{A}^T\boldsymbol{W}\boldsymbol{A}\right)^{-1}\boldsymbol{A}^T\boldsymbol{W}\boldsymbol{R}\boldsymbol{W}\boldsymbol{A}\left(\boldsymbol{A}^T\boldsymbol{W}\boldsymbol{A}\right)^{-1}\right] \tag{36}$$

Defining the weighting matrix $\boldsymbol{W}$ to be the inverse of $\boldsymbol{R}$:

$$\boldsymbol{R} = \boldsymbol{W}^{-1} \tag{37}$$

$$\boldsymbol{P}_{\delta\boldsymbol{x}_n} = E\left[\left(\boldsymbol{A}^T\boldsymbol{W}\boldsymbol{A}\right)^{-1}\boldsymbol{A}^T\boldsymbol{W}\boldsymbol{W}^{-1}\boldsymbol{W}\boldsymbol{A}\left(\boldsymbol{A}^T\boldsymbol{W}\boldsymbol{A}\right)^{-1}\right] \tag{38}$$

$$\boldsymbol{P}_{\delta\boldsymbol{x}_n} = \left(\boldsymbol{A}^T\boldsymbol{W}\boldsymbol{A}\right)^{-1} \tag{39}$$

To find a unitless PDOP metric that is multiplied by the range measurement noise, the ratio between the range and range-rate noise k is defined:

$$k = \frac{\sigma_r}{\sigma_{\dot{r}}} \tag{40}$$

The weighting matrix can thus be expressed using k:

$$\boldsymbol{W} = \frac{1}{\sigma_r^2}\boldsymbol{K} \tag{41}$$

Where $\boldsymbol{K}$ is:

$$\boldsymbol{K} = \begin{bmatrix} 1 & 0 \\ 0 & k^2 \end{bmatrix} \tag{42}$$

The value σ_r^2 is factored out of the inverse:

$$\boldsymbol{P}_{\delta \boldsymbol{x}_n} = \sigma_r^2 \left(\boldsymbol{A}^T \boldsymbol{K} \boldsymbol{A} \right)^{-1} \tag{43}$$

$$\text{RSS}(\boldsymbol{P}_{\delta \boldsymbol{r}_n}) = \sigma_r \sqrt{\text{tr} \left[\boldsymbol{M_r}^T \left(\boldsymbol{A}^T \boldsymbol{K} \boldsymbol{A} \right)^{-1} \boldsymbol{M_r} \right]} \tag{44}$$

$$\boxed{\text{RSS}(\boldsymbol{P}_{\delta \boldsymbol{r}_n}) = \sigma_r \text{PDOP}} \tag{45}$$

Note this PDOP is also a dimensionless quantity, but is formulated by using both range and range-rate data. Also note that if a dimensionless VDOP were desired, the range-rate measurement noise could be factored out in a way similar to Eq. 41 and the matrix $\boldsymbol{K}$ redefined. As before, a recursive algorithm is developed to process new measurements:

$$\boxed{\left[\boldsymbol{A}^T \boldsymbol{K} \boldsymbol{A} \right]_{i+1} = \boldsymbol{H}_{i+1}^T \boldsymbol{K} \boldsymbol{H}_{i+1} + \boldsymbol{\Phi}_{i,i+1}^T \left[\boldsymbol{A}^T \boldsymbol{K} \boldsymbol{A} \right]_i \boldsymbol{\Phi}_{i,i+1}} \tag{46}$$

And applying the matrix inversion lemma:

$$\boldsymbol{\Gamma}_i = \left[\boldsymbol{A}^T \boldsymbol{K} \boldsymbol{A} \right]_i^{-1} \tag{47}$$

$$\boldsymbol{\Gamma}_{i+1}^- = \boldsymbol{\Phi}_{i+1,i} \boldsymbol{\Gamma}_i \boldsymbol{\Phi}_{i+1,i}^T \tag{48}$$

$$\boxed{\boldsymbol{\Gamma}_{i+1}^+ = \boldsymbol{\Gamma}_{i+1}^- - \boldsymbol{\Gamma}_{i+1}^- \boldsymbol{H}_{i+1}^T \left(\boldsymbol{I} + \boldsymbol{K} \boldsymbol{H}_{i+1} \boldsymbol{\Gamma}_{i+1}^- \boldsymbol{H}_{i+1}^T \right)^{-1} \boldsymbol{K} \boldsymbol{H}_{i+1} \boldsymbol{\Gamma}_{i+1}^-} \tag{49}$$

The first recursion method in Eq. 46 is used until the condition number tolerance is met, then $\boldsymbol{\Gamma}$ is calculated and the second recursion method in Eq. 49 is implemented, as depicted in Fig. 4:

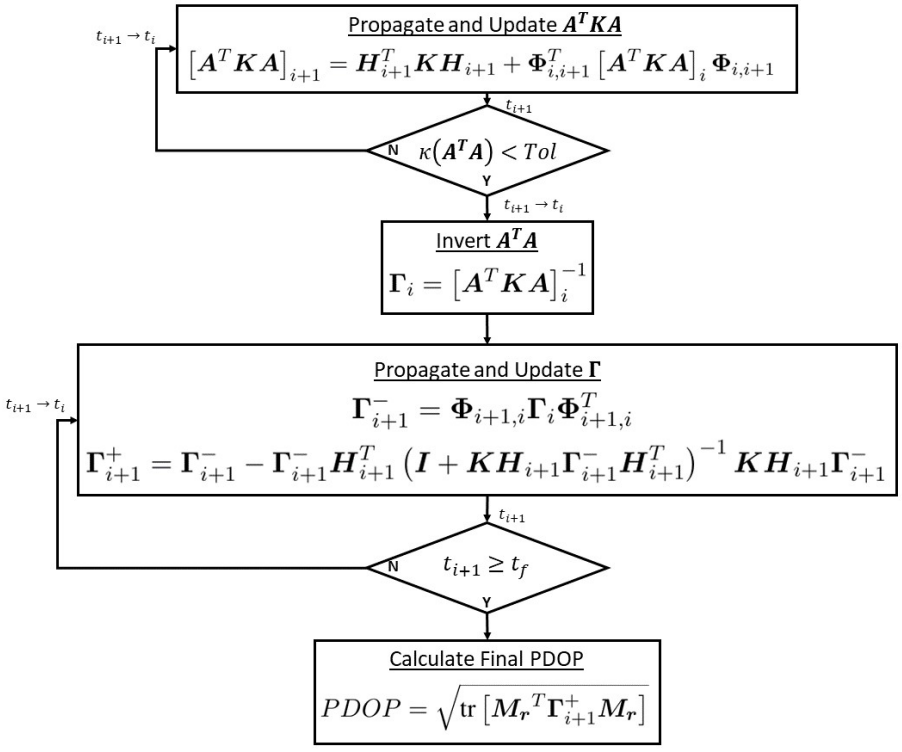

Figure 4: DOP Algorithm Flow Chart: Multi-Measurement Incorporation

Thus a recursive, multi-measurement DOP algorithm has been explicitly derived that may be used to quickly analyze the performance of a ground station tracking schedule. A significant benefit of DOP analysis over other estimation algorithms is that the DOP algorithm saves on runtime by strictly analyzing the dynamic measurement geometry by assuming the dominate sources of uncertainty are in the spacecraft's position and velocity. When other sources of uncertainty become important, e.g., large measurement biases, large uncertainty in SRP, or other large random accelerations, other estimation techniques should be considered for ground station tracking optimization.

Another advantage of the DOP algorithm is that it does not require explicit information regarding the measurement noise. For the DOP algorithm containing one measurement type, the algorithm is independent of the measurement noise. The DOP algorithm implementing two measurement types requires a more general knowledge of the ratio between range and range-rate noise. For ground-based range and range-rate measurements, this ratio k is generally between 1×10^3 and 1×10^5. For the optimization studies here, a value of $k = 1 \times 10^5$ is used.

GENETIC ALGORITHM OPTIMIZATION SETUP

Optimization Object

The Optimization Object is the set of parameters that the optimization algorithm alters to minimize the PDOP objective function. The Optimization Object contains information on which stations are used and the operation times. In order to ensure near-continuous station coverage and minimize the number of elements in the Optimization Object, the time variable is the swap time between stations. For example, if an optimal tracking schedule with two stations were desired, the Optimization Object would be:

$$\boldsymbol{s} = \begin{bmatrix} N_1 & N_2 & t_{1:2} \end{bmatrix}^T$$

Where N_1 and N_2 are any of the ten available stations, and $t_{1:2}$ indicates the time when tracking swaps from station N_1 to N_2. For an optimal tracking schedule with three stations, the Optimization Object would be:

$$\boldsymbol{s} = \begin{bmatrix} N_1 & N_2 & N_3 & t_{1:2} & t_{2:3} \end{bmatrix}^T$$

Where N_1, N_2, and N_3 are any of the ten available stations, $t_{1:2}$ indicates the time when tracking swaps from station N_1 to N_2, and $t_{2:3}$ indicates the time when tracking swaps from station N_2 to N_3. This pattern is generalized to include any number of stations to an OD segment with the Optimization Object:

$$\boldsymbol{s} = \begin{bmatrix} N_1 & N_2 & \cdots & N_n & t_{1:2} & t_{2:3} & \cdots & t_{(n-1):n} \end{bmatrix}^T$$

where the size of the Optimization Object depends on the number of stations to be considered for an OD segment. The total size of the Optimization Object is (2*N*-1) with *N* stations and *N-1* swap times.

Formulating the Optimization Object with the swap time variables as opposed to start and stop time variables is advantageous in a few ways. First, the size of the Optimization Object reduces from 3*N* with separate start and stop time variables to (2*N*-1) with swap time variables, which helps the speed of the optimization algorithm. Second, the swap time variables encourage the formulation of continuous coverage tracking schedules. Additional measurements will never worsen estimation performance, meaning the optimal solution will be as close to continuous coverage as possible. Lastly, a continuous tracking schedule is desired by Intuitive Machines for the IM-1 mission. For

future missions, tracking schedules with less coverage may be desired to save on operational costs. Operational costs are discussed in a later section and can be implemented into the objective function to produce optimal tracking schedules by minimizing other metrics besides PDOP.

The optimization problem at hand is an integer problem, since the station numbers must be integer values 1-10 mapping to an actual station, with swap times at discrete 30 minute increments. While the ground stations are assumed to provide measurements every 10 seconds, the discretization of the swap times does not need to be so precise. By discretizing the swap times at 30 minute increments, the number of possible combinations for the Optimization Object dramatically decreases. For example, a 20 hour OD segment that has three stations and a swap time discretization set at 10s has over 13.64 trillion combinations. By discretizing the swap times at 30 minute increments, the number of possible configurations decreases to just over 171,000.

Optimization Procedure using a Genetic Algorithm

Genetic algorithms are well suited to find the best Optimization Object for integer problems with complex objective functions.[13,14] Using MATLAB's genetic algorithm optimization toolbox,[15] the genetic algorithm creates an initial population of Optimization Objects. From each of these Optimization Objects, a ground station tracking schedule is created and run through the DOP algorithm to obtain the PDOP at the final time. The genetic algorithm creates new Optimization Objects based on the previous population and iterates until an optimal ground station tracking schedule is found. The optimization process is depicted in Fig. 5:

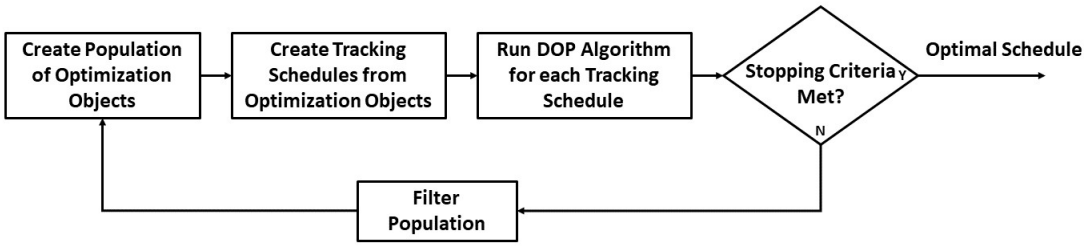

Figure 5: Ground Station Tracking Schedule Optimization Procedure

The stopping criteria include run time, number of generations, and function tolerance, where the genetic algorithm terminates if any one of the criteria is met. The genetic algorithm is applied to each OD segment and subsegment in cislunar space to find an optimal ground station tracking schedule with three stations in the Optimization Object. With three ground stations, each OD segment is "well covered" in terms of having continuous coverage. The inclusion of subsequent stations to the Optimization Object yields smaller marginal gains in DOP performance with increasing complexity for the genetic algorithm. However, including more stations decreases the PDOP and may be necessary to ensure mission success.

To help the genetic algorithm find optimal tracking schedules with more than three stations, an initial population is fed into the genetic algorithm based on the optimal three station configuration. This process is iterated to find optimal tracking schedules that contain four, five, and six stations. Doing so, while also introducing random elements to the initial population, helps the genetic algorithm converge more consistently to the optimal solution in a faster time. Lastly, the optimal solutions are fed back into a genetic algorithm to increase the precision of the swap times.

It is important to note that as the number of stations in the Optimization Object increases, the confidence that the genetic algorithm provides the global minimum decreases. For a 20 hour OD segment with the half-hour time discretization, there exist over 3.2 billion potential solutions for six stations. For continuous coverage, millions of these configurations could produce PDOP values that are near the global minimum, and the genetic algorithm may have difficulty converging to the global solution due to numerical precision. Furthermore, local minima are always a concern for non-convex optimization problems. To ensure the genetic algorithm approaches the global minimum, a very large initial population is implemented that attempts to span the entire sample space. The genetic algorithm is also run multiple times to ensure consistent solution convergence. Ultimately, the differences between the PDOP found by the genetic algorithm and the true global minimal PDOP should be minimal.

For the OD segments and subsegments in cislunar space, optimal ground station tracking schedules are found for three to six stations in the Optimization Object. For lunar orbit, the subsegments are much shorter and the dynamics are dominated by the lunar two-body problem, thus an optimal tracking schedule with only two stations in the Optimization Object is found.

Operational Costs and Nav-Dollars

Another element considered in this research is the operational cost of each the tracking schedule. Each ground station is assigned a weighted dollar value (selected from 1, 2, and 2.5) that represents the cost to operate the ground station during measurement generation. The operational cost for a station is calculated by multiplying the station's operation time by its weighted dollar value. Thus, measurements taken from a station with operational weight of 2 would cost twice as much as measurements taken during the same interval from a station with an operational weight of 1.

With each station assigned different weights, the total operational cost of the optimal tracking schedules is calculated by summing the individual operational cost of each station. The results shown are in units of dollar, but should not be treated as real dollar estimates. Operational costs provide insight into whether an additional station is worth the DOP improvement. The best case scenario is a tracking schedule that minimizes both PDOP and operational costs. However, the more common scenario is an additional station decreases the PDOP, but increases operational costs. To analyze the trade off between PDOP and operational costs, the two values are multiplied together to provide a combined metric, referred to as Nav-Dollars.

The Nav-Dollar metric comes from maximizing the information per dollar obtained through a tracking schedule. Optimization traditionally attempts to minimize a cost function, so the inverse of information per dollar is minimized, which can be calculated by dividing the operational cost by the information obtained from a tracking schedule. Since PDOP is derived from the inverse of the information matrix, minimizing the product of PDOP and operational costs, referred to as Nav-Dollars, is equivalent to maximizing position information per dollar.

Since PDOP is unitless, the Nav-Dollars metric also has units of dollars. The operational cost estimate and the Nav-Dollars metric are displayed for each OD segment, but the DOP is always the objective function of the genetic algorithm. Future work will be performed to produce ground station tracking schedules that optimize Nav-Dollars.

RESULTS: GROUND STATION TRACKING SCHEDULES FOR CISLUNAR SPACE

Benchmark Configurations

To further demonstrate how the optimal ground station tracking schedules perform, a benchmark configuration is provided by Intuitive Machines for cislunar space. The benchmark tracking schedule prioritizes 6 stations: Hartebeesthoek, South Africa (HBK26); Kourou, French Guiana (KRU1); Byalulu, India (D32); Okinwawa, Japan (OKN2); Morehead, Kentucky (DSS17); Goonhilly, England (GHY6). These 6 stations are able to provide tracking at any given distance in cislunar space.

The number of stations in each OD segment and subsegment is not constant in the benchmark schedule, containing either 4 or 5 stations in all OD subsegments except during lunar approach from TCM2H-TCM3, which has 3 stations. The benchmark schedule may perform better than the optimal configuration due to having more stations, however when the OD segments have the same number of stations the optimal configuration will have a lower PDOP than the benchmark.

Optimization Results

The optimal PDOP results for each of the OD subsegments in cislunar space are depicted below in Table 1:

Table 1: Cislunar Optimal PDOP Results

OD Segment:	OD1	OD2.1	OD2.2	OD3.1	OD3.2	OD4.1	OD4.2	OD5
Benchmark:	.10656	.71524	.59872	.68996	.88401	.84967	.86710	.87859
3 Stations:	.10730	.32776	.44037	.54124	.56685	.60292	.60669	.28443
4 Stations:	.09756	.29023	.40999	.49464	.51556	.55772	.55029	.27266
5 Stations:	.09572	.27533	.39999	.47007	.49215	.52816	.52773	.26742
6 Stations:	.09285	.27386	.38877	.45103	.48683	.51499	.52103	.26152

Note that for all OD subsegments, except for OD1, the optimal tracking schedule with just 3 stations outperforms the benchmark, despite having fewer stations. The optimal schedule with 3 stations in OD1 is the only optimal schedule that does not outperform the benchmark, which has 5 stations. However, the difference is minimal and the addition of the fourth station to the optimal solution outperforms the benchmark.

Also note that improvement in PDOP decreases in smaller margins as the number of stations increases in the optimal solution. For example, the 3 station optimal schedule for OD2.1 experiences a .38748 PDOP improvement from the benchmark. As stations are added, the improvement is only an additional .03753 with a fourth station, .01490 with a fifth station, and .00147 with a sixth station. Given this pattern, the inclusion of a seventh station to the optimal schedule is not included in this research.

Patterns in Optimal Tracking Schedules

Figure 6 below depicts the benchmark and optimal tracking schedules for two OD subsegments, corresponding to OD segment OD2.1, CM-TCM1. Note that only six stations are used, as the other dishes are limited by their range capabilities.

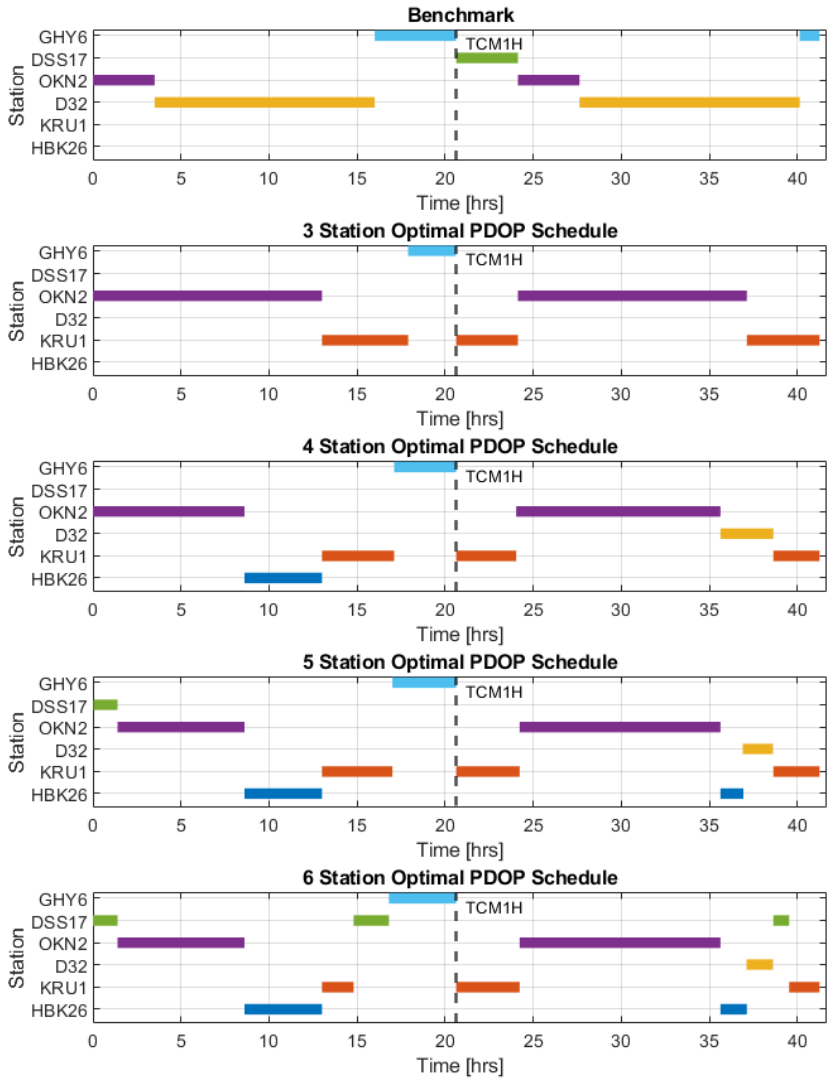

Figure 6: CM-TCM1 Tracking Schedules

Note that swapping between stations that vary significantly in latitude and/or longitude improves the dynamic measurement geometry, lowering PDOP. Note how large longitude swaps occur when the schedule swaps from OKN2 to KRU1, and large latitude swaps occur when the schedule swaps from KRU1 or HBK26 to GHY6. Furthermore, note that OKN2 is used for the most time as Okinawa, Japan is the only station visible as the spacecraft is over the pacific ocean. Thus utilizing constant station coverage with stations that vary with latitude and longitude improves station geometry. Also note that frequently additional optimal stations are added in near the end of the OD subsegment. This occurs as the optimizer focuses on minimizing PDOP at the final time.

Operational Costs and Nav-Dollars Comparison

While the PDOP may decrease in smaller margins with additional stations in the optimization, the PDOP improvement may be worth the cost of operating the tracking schedule. The smaller gains in PDOP are put into context by analyzing the operational costs and Nav-Dollars for each OD subsegment. The operational costs and Nav-Dollars for each OD subsegment, along with the PDOP, are shown below in Table 2:

Table 2: Operational Costs and Nav-Dollars

OD Segment:	OD1	OD2.1	OD2.2	OD3.1	OD3.2	OD4.1	OD4.2	OD5
Benchmark:								
PDOP:	.10656	.71524	.59872	.68996	.88401	.84967	.86710	.87859
Operational Costs:	10,974	8,879	10,093	10,035	9,998	9,973	9,634	6,480
Nav-Dollars:	1,169	6,351	6,043	6,923	8,838	8,474	8,354	5,693
3 Stations:								
PDOP:	.10730	.32776	.44037	.54124	.56685	.60292	.60669	.28443
Operational Costs:	16,530	13,286	13,775	11,274	10,586	10,414	13,347	10,910
Nav-Dollars:	1,774	4,355	6,066	6,102	6,001	6,279	8,097	3,103
4 Stations:								
PDOP:	.09756	.29023	.40999	.49464	.51556	.55772	.55029	.27266
Operational Costs:	14,460	14,815	13,602	11,263	12,287	13,073	15,578	12,256
Nav-Dollars:	1,411	4,300	5,576	5,571	6,335	7,291	8,572	3,342
5 Stations:								
PDOP:	.09572	.27533	.39999	.47007	.49215	.52816	.52773	.26742
Operational Costs:	14,576	15,013	14,250	10,802	12,171	13,704	14,517	12,114
Nav-Dollars:	1,395	4,133	5,700	5,078	5,990	7,238	7,661	3,239
6 Stations:								
PDOP:	.09285	.27386	.38877	.45103	.48683	.51499	.52103	.26152
Operational Costs:	15,431	14,572	14,178	13,319	12,044	14,801	15,003	12,256
Nav-Dollars:	1,433	3,991	5,512	6,015	5,863	7,622	7,817	3,205

The results in Table 2 indicate some general trends. The benchmark schedule has the lowest operational costs across all OD subsegments, but does not always have the lowest Nav-Dollars. For OD1, the benchmark outperforms all of the optimal schedules in operational costs and Nav-Dollars. This is due to the fact that the optimal schedules experience minimal gains in PDOP for a higher operational cost. This OD segment alone is a strong motivation to generate tracking schedules that minimize Nav-Dollars as opposed to PDOP.

The results in Table 2 also indicate that operational costs are generally lower when fewer stations are used. Table 3 shows the complete tracking schedule for cislunar space that minimizes operational costs, based on the optimal minimization of PDOP:

Table 3: Lowest Operational Cost Tracking Schedules Based on Optimal PDOP Solutions

OD Segment:	OD1	OD2.1	OD2.2	OD3.1	OD3.2	OD4.1	OD4.2	OD5
Number of Stations:	4	3	4	5	3	3	3	3
Operational Cost:	14,460	13,286	13,602	10,802	10,586	10,414	13,347	10,910
Optimal PDOP:	.09756	.32776	.40999	.47007	.56685	.60292	.60669	.28443

Table 3 indicates that for five out of eight OD subsegments, the operational costs are minimized when the optimal three station schedules are used. Furthermore, optimal schedules with six stations are not used to minimize operational costs at all. This supports the intuition that adding more stations, and subsequently covering more of the OD subsegment, increases operational costs. However, some schedules in Table 3 contain four or five stations. This occurs when an optimal schedule with fewer stations utilizes a more expensive station, and the inclusion of an additional, less expensive station lowers PDOP while also reducing the time the more expensive station is used.

Table 2 does not however indicate any pattern between the number of stations used and Nav-Dollars. As previously mentioned, Nav-Dollars measures the combination of PDOP and operational costs, measuring the cost of producing smaller PDOP values and thus better estimation solutions. Thus, while using fewer stations is generally less expensive, the additional station may be worth the extra cost in order to significantly reduce the PDOP. Table 4 shows the tracking schedule in cislunar space that minimizes Nav-Dollars, based on the optimal minimization of PDOP.

Table 4: Lowest Nav-Dollar Tracking Schedules Based on Optimal PDOP Solutions

OD Segment:	OD1	OD2.1	OD2.2	OD3.1	OD3.2	OD4.1	OD4.2	OD5
Number of Stations:	4	6	6	5	6	3	5	3
Nav-Dollars:	1,411	3,991	5,512	5,078	5,863	6,279	7,661	3,103
Optimal PDOP:	.09572	.27386	.38877	.47007	.48683	.60292	.52773	.28443

Table 4 indicates that the Nav-Dollars are minimized by using varying number of stations per OD subsegment. As previously mentioned, future work will be done to find optimal ground station tracking schedules that minimize Nav-Dollars since may schedules may exist that produce similar PDOP values close the minimum for a lower operational cost.

RESULTS: GROUND STATION TRACKING SCHEDULES FOR LUNAR ORBIT

The benchmark schedule in lunar orbit is generated by analyzing each OD subsegment with only one station and selecting the station that minimizes PDOP. This is performed by simply testing each station per OD subsegment and does not require the genetic algorithm. The benchmark and the optimal ground station tracking schedule with two stations per OD subsegment in lunar orbit are depicted in Fig. 7:

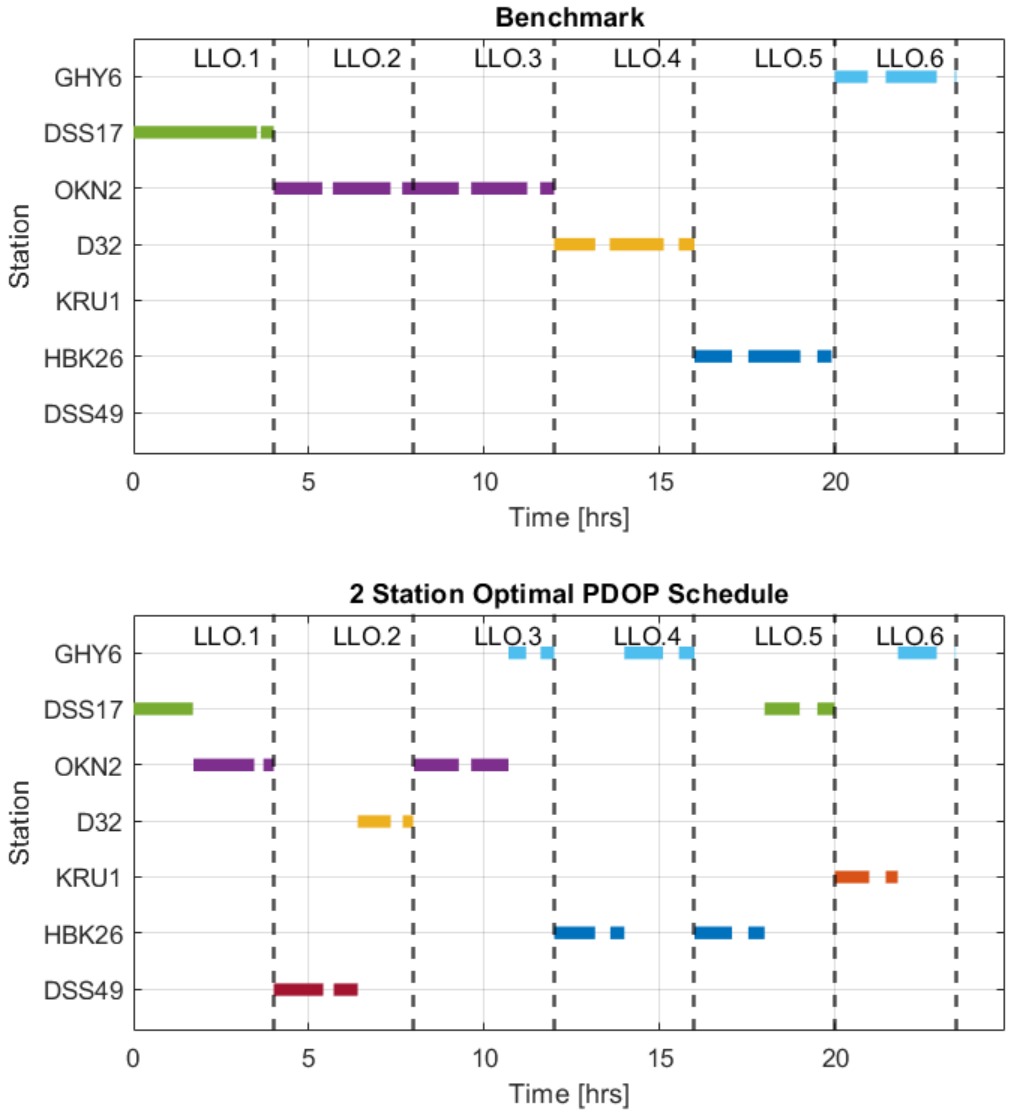

Figure 7: Optimal Two Station Schedule

Table 5 shows the PDOP for each OD subsegment and the comparison to the benchmark.

Table 5: Optimal Two Station Schedule Values

OD Segment:	LLO.1	LLO.2	LLO.3	LLO.4	LLO.5	LLO.6
Benchmark PDOP:	.05878	.08983	.06530	.06760	.09110	.09599
Optimal PDOP:	.02376	.02694	.02563	.01990	.01963	.02949
Percent Improvement:	59.6%	70.0%	60.6%	70.6%	78.5%	69.3%

Note that with just one station per OD subsegment, the PDOP values are considerably small. This is due to the well defined dynamics in lunar orbit causing less severe uncertainty propagation and better state estimation. Also note the significant improvement in the PDOP with the additional station, ranging from 59.6% to 78.45% improvement. Due to the significantly small values of PDOP, the addition of a third station is not considered in this research.

An analysis of the operational costs, shown in Table 6 shows that for all OD subsegments in lunar orbit, the two station configuration outperforms the one station benchmark:

Table 6: Operational Costs for 2 Station Optimal PDOP

OD Segment:	LLO.1	LLO.2	LLO.3	LLO.4	LLO.5	LLO.6
Benchmark Operational Costs:	2,486	2,350	2,282	1,098	2,349	925
Optimal Schedule Operational Costs:	2,614	1,294	1,973	1,924	2,382	1,619

An analysis of the Nav-Dollars, shown in Table 7 shows that for all OD subsegments in lunar orbit, the two station configuration outperforms the one station benchmark:

Table 7: Nav-Dollars for 2 Station Optimal PDOP

OD Segment:	LLO.1	LLO.2	LLO.3	LLO.4	LLO.5	LLO.6
Benchmark Nav-Dollars:	146	211	149	74	214	89
Optimal Nav-Dollars:	62	35	51	38	47	48

For OD subsegments LLO.1 and LLO.5 the operational costs are similar, but the PDOP performance is drastically better in the optimal schedule with two stations resulting in significantly lower Nav-Dollars. In lunar orbit, all of the OD subsegments exhibit significantly better Nav-Dollars than the one station benchmark. Thus using two stations is favorable in terms of PDOP performance and in Nav-Dollars.

CONCLUSION AND FUTURE WORK

In conclusion, the research in this paper derived and implemented a recursive DOP algorithm to maximize OD performance by finding optimal ground station tracking schedules. The DOP algorithm incorporated the system dynamics due to the point mass gravitational pull from the Earth, Moon, and Sun and implemented measurement data from both range and range-rate data to output the dimensionless PDOP metric. A genetic algorithm was used to find optimal ground station tracking schedules that minimized PDOP for key OD segments in the IM-1 nominal trajectory, including segments in cislunar space and in lunar orbit. The optimal tracking schedules were also analyzed using Nav-Dollars to study the trade-off between OD performance and operational costs.

The DOP algorithms demonstrate great potential for rapid dynamics measurement geometry assessment, particularly for ground station tracking schedule optimization. The genetic algorithm and the DOP algorithm can be applied to any nominal trajectory in order to minimize state estimation errors, not just for cislunar operations.

Future work will be performed to create optimal tracking schedules to minimize Nav-Dollars. Due to the near continuous coverage from multiple stations, a PDOP that is near the global minimum may exist for a much lower operational cost, which can be found using Nav-Dollars. Furthermore, the results presented in this research were for the noise ratio $k = 1 \times 10^5$, when different values of k will produce different optimal tracking schedules.

CONFLICT OF INTEREST STATEMENT

On behalf of all authors, the corresponding author states that there is no conflict of interest.

REFERENCES

[1] L. J. Wood, "The evolution of deep space navigation: 1962-1989," *AAS*.

[2] B. Cockrell, "RTCC requirements for mission G-Lunar module attitude determination using onboard observation. Project Apollo," tech. rep., 1968.

[3] C. Christensen and S. Reinbold, "Navigation of the Mariner 10 spacecraft to Venus and Mercury," *Mechanics and Control of Flight Conference*, 1974, p. 844.

[4] R. Russell and J. Ellis, "Orbit determination for a Jupiter Orbiter Tour of the Galilean satellites," *Journal of Spacecraft and Rockets*, Vol. 12, No. 6, 1975, pp. 368–373.

[5] B. v. Noort, "The Gravity of Titan: Analysis of Cassini's Doppler Tracking Data and Solar Radiation Pressure," 2021.

[6] R. H. Battin, *An introduction to the mathematics and methods of astrodynamics*. Aiaa, 1999.

[7] P. Axelrad, R. Brown, B. Parkinson, and J. Spilker, "GPS navigation algorithms," *Global Positioning System: Theory and applications.*, Vol. 1, 1996, pp. 409–433.

[8] O. S. Sands, J. W. Connolly, B. W. Welch, J. R. Carpenter, T. A. Ely, and K. Berry, "Dilution of precision-based lunar navigation assessment for dynamic position fixing," *Proceedings of the 2006 National Technical Meeting of The Institute of Navigation*, 2006, pp. 260–268.

[9] Q. Moon, D. Geller, *et al.*, "Validation of Linear Covariance Analysis for NOVA-C Cislunar Trajectory Design: https://www.researchgate.net/publication/370805481_Preprint_AAS_22-023_VALIDATION_OF_LINEAR_COVARIANCE_ANALYSIS_FOR_NOVA-C_CISLUNAR_TRAJECTORY_DESIGN/references," 2022.

[10] J.-R. Carpenter and C. N. D'Souza, "Navigation filter best practices," tech. rep., 2018.

[11] T. Moon and W. Stirling, *Mathematical Methods and Algorithms for Signal Processing*. Prentice Hall, 2000.

[12] P. S. Maybeck, *Stochastic models, estimation, and control*. Academic press, 1982.

[13] J. H. Holland, "Genetic algorithms," *Scientific american*, Vol. 267, No. 1, 1992, pp. 66–73.

[14] A. Wuerl, T. Crain, and E. Braden, "Genetic algorithm and calculus of variations-based trajectory optimization technique," *Journal of spacecraft and rockets*, Vol. 40, No. 6, 2003, pp. 882–888.

[15] T. M. Inc., "MATLAB version: 9.13.0 (R2022b)," 2022.